Crystal Structure Determination of Poly(1,4-*trans*-cylcohexylenedimethylene 2,6-naphthalate) by X-ray Diffraction and Molecular Modeling

Young Gyu Jeong and Won Ho Jo*

Hyperstructured Organic Materials Research Center and School of Materials Science and Engineering, Seoul National University, Seoul 151-742, Korea

Sang Cheol Lee

School of Material and System Engineering, Kumoh National University of Technology, Kumi 730-701, Korea

Received October 8, 2002; Revised Manuscript Received April 28, 2003

ABSTRACT: The crystal structure of poly(1,4-*trans*-cyclohexylenedimethylene 2,6-naphthalate) (P*t*CN) was identified by X-ray diffraction and molecular modeling, and the effect of the *trans*/*cis* ratio of 1,4-cyclohexylenedimethyl unit on the crystal structure of P*t*CN was also investigated. The unit cell of P*t*CN is found to be a triclinic with dimensions of $a = 0.638$ nm, $b = 0.657$ nm, $c = 1.661$ nm, $\alpha = 83.41°$, $\beta = 43.92°$, and $\gamma = 106.02°$, and the space group of the crystal is identified as $P\bar{1}$. The calculated crystal density of 1.313 g/cm^3 indicates that there is one repeating unit in a unit cell. The crystal structure of P*t*CN was also determined by using the molecular modeling technique and then confirmed by comparing the calculated structure factors with the ones obtained from the X-ray fiber diagram. The flexible unit, a 1,4-*trans*-cyclohexylenedimethoyl group [−O−CH_2−(C_6H_{10})−CH_2−O−] in the P*t*CN backbone, is in the conformation of t^{t}_{+g} $(t \pm gt)^{-g}_{t}t$ (*g*, *gauche*; *t*, *trans*), and the naphthalene rings are in a face-to-face arrangement. It was observed that the crystal structures of polymers containing above 70% 1,4-*trans*-cyclohexylenedimethyl groups are nearly the same as that of the crystal structure of P*t*CN.

Introduction

Since aromatic polyesters derived from various diols and diacids show good thermal and mechanical properties, they have attracted much interest for a long time. Among those aromatic polyesters, poly(*m*-methylene 2,6-naphthalatates) (P*m*N, *m* is the number of methylene units) with the chemical structure as shown in Figure 1a have recently attracted attention from both academia and industry, since those were first reported in 1969.[1] Particularly, since 2,6-naphthalenedicarboxylic acid (NA) has been recently produced in a large-scale quantity, the P*m*N family based on this monomer has high potential to be used as commercial engineering plastics.

The most well-known polymer among this P*m*N family is poly(ethylene 2,6-naphthalate) (PEN, $m = 2$), whose crystal structures, thermal properties, and mechanical properties have widely been studied. It has been reported that PEN has two crystal structures, i.e., α-form and *β*-form, depending upon the crystallization temperature.[2−4] The α-form has a triclinic unit cell with a fully extended chain, and the *β*-form has also a triclinic unit cell containing four chains with non-*trans* conformation. It has also been reported that poly(butylene 2,6-naphthalate) (PBN, $m = 4$) exhibits two crystal structures, i.e., A-form and B-form, depending upon the crystallization temperature and the applied stress.[5,6] The major difference between two crystal structures is seen in the fiber period (*c*-axis) due to the difference in the molecular conformation of the butylene units as in the case of poly(butylene terephthalate); i.e., the main chain in the B-form crystal is more extended than that in the A-form crystal. Recently, we have identified the crystal structures of poly(trimethylene 2,6-naphthalate) (PTN, $m = 3$), poly(pentamethylene 2,6-naphthalate) (PPN, $m = 5$), and poly(hexamethylene 2,6-naphthalate) (PHN, $m = 6$).[7−10] It was found that both PTN and PHN have also two crystal structures, α-form and *β*-form, depending upon the crystallization temperature, whereas PPN with a triclinic unit cell does not show polymorphism by the temperature or external stress. Trimethylene units of PTN in both crystal structures take the *gauche*/*gauche* conformation, and the middle part of pentamethylene units of PPN in the unit cell also takes the *gauche*/*gauche* conformation, whereas hexamethylene units in both crystal structures of PHN take the nearly *all-trans* conformation.

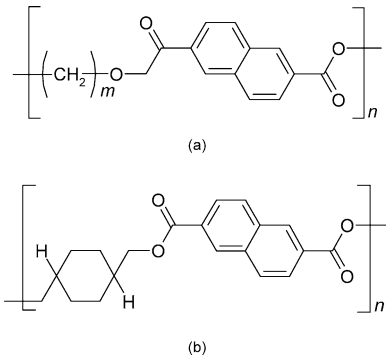

Figure 1. Chemical structures of (a) poly(*m*-methylene 2,6-naphthalate) (P*m*N) and (b) poly(1,4-cyclohexylenedimethylene 2,6-naphthalate) (PCN).

When a rigid and thermally stable cycloaliphatic diol, 1,4-cyclohexanedimethanol (CHDM), is used instead of

* To whom correspondence should be addressed: Tel 82-2-880-7192; Fax 82-2-885-1748; e-mail whjpoly@plaza.snu.ac.kr.

10.1021/ma0215666 CCC: $25.00
Published on Web 06/20/2003

the above linear aliphatic diols in synthesizing aromatic polyesters, it is expected that the new polyester synthesized from CHDM and NA may have better thermal and mechanical properties. The CHDM monomer has been commercially produced in a mixture of *trans*/*cis* (70/30) isomers. Based on CHDM, poly(1,4-cyclohexylenediemthylene terephthalate) (PCT) has been commercially produced and widely used as an engineering plastic. However, poly(1,4-cyclohexylenedimethylene 2,6-naphthalate) (PCN), which has the chemical structure similar to that of PCT except a benzene ring in PCT replaced by a naphthalene ring, as shown in Figure 1b, has not been reported yet.

In the present study, we have synthesized several kinds of PCN samples with various *trans*/*cis* ratios of CHDM and identified the crystal structure of poly(1,4-*trans*-cyclohexylenedimethylene 2,6-naphthalate) (P*t*CN) using X-ray diffraction and molecular modeling. The effect of the *trans*/*cis* ratio of 1,4-cyclohexylenedimethyl unit on the crystal structure of P*t*CN was also studied by X-ray diffraction.

Experimental Section

Synthesis of PCN. CHDM monomers with different *trans*/*cis* ratios were prepared by fractionally distilling commercially available CHDM (*trans*/*cis* = 70/30) at a temperature of 155 °C under a reduced pressure in the presence of aqueous solution of NaOH.[11] The fractional distillation yields CHDMs with various *trans* isomer fractions of 70.1, 80.8, 90.5, and 96.4%. The isomer composition of *trans*/*cis*-CHDM was determined by using a gas chromatograph with mass selective detector. PCNs were synthesized by melt-condensation of CHDMs with dimethyl-2,6-naphthalate (DMN) using tetraisopropyl orthotitanate as a catalyst. Two-step polymerization was performed on a laboratory-scale polymerization reactor in the melt state. The first step was the transesterification reaction of CHDM with DMN, and the second was the polycondensation reaction. The transesterification reaction was carried out at 230−280 °C under a nitrogen atmosphere, and the extent of the reaction was monitored by measuring the amount of methanol evolved. The polycondensation was carried out at 330−350 °C under high-vacuum conditions. At the end of the reaction, the product in the melt was quenched into water bath and followed by drying in a vacuum oven for several days.

PCN monofilaments of 1.0 mm in diameter were prepared by using a capillary rheometer (D8052B, Kayeness Inc.) and were drawn to the strain of 400% at 170 °C on a universal tensile machine (LR 10K, Lloyd Inc.) with the cross-head speed of 1 cm/min. The monofilaments were further annealed at 250−300 °C under tension with nitrogen gas purging to minimize oxidative degradation. Amorphous and crystalline PCN films were prepared by heating the sample to the temperature 30 °C higher than the melting temperature, holding for 3 min in order to melt completely crystals, and rapidly transferring into cooling water or into another hot plate set at the predetermined crystallization temperature, respectively.

Characterization of PCN Samples. The intrinsic viscosities of all samples were determined in a mixed solvent of phenol/1,1,2,2-tetrachloroethane (6/4, v/v) at 35 °C with an Ubbelohde capillary viscometer. ^{1}H NMR spectroscopy was used for determining the *trans*/*cis* ratio of 1,4-cycloehaxedimethyl groups in PCN samples. The ^{1}H NMR spectra of $CDCl_3$/CF_3COOD solutions were recorded on a Bruker AMX500 operating at 500 MHz. Thermal properties of the samples were measured with a Perkin-Elmer DSC-7 differential scanning calorimeter equipped with an intercooler at a heating rate of 20 °C/min. DSC heating thermograms of the melt-quenched amorphous PCNs show that PCNs synthesized in this study have high glass transition (>110 °C) and high melting (>320 °C) temperatures, as shown in Figure 2. It also shows that

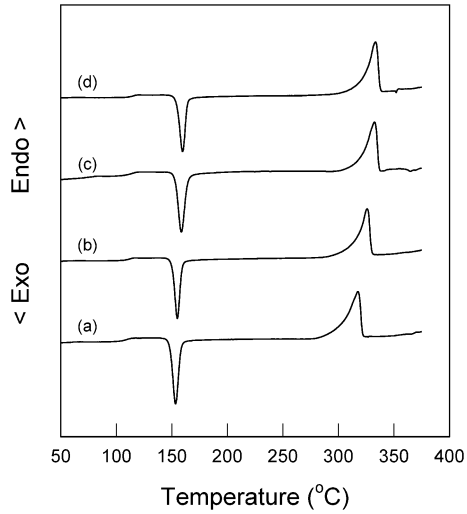

Figure 2. DSC heating thermograms of the melt-quenched amorphous PCN samples: (a) PCN-70; (b) PCN-82; (c) PCN-90; (d) PCN-97.

the glass transition and melting temperatures of PCNs increase with increasing the isomer fraction of *trans*-CHDM. Characteristics of PCN samples synthesized in this study are listed in Table 1. Intrinsic viscosities of the samples are around 0.5 dL/g, indicating that the synthesized PCNs have high molecular weight enough to form in monofilament or in film. The density (ρ_1) of sample was calculated using the equation of $\rho_1 = A\rho_0/(A - B)$, where A and B denote the weight of sample measured in air and in distilled water, respectively, and ρ_0 is the density of distilled water. Weights of sample in air and in distilled water were measured using a Mettler AT200 balance (Mettler-Toledo Inc.).

X-ray Diffraction. The X-ray fiber diagrams of monofilaments uniaxially drawn and annealed were recorded on a DIP2030 X-ray system (MAC Science Co.) with the flat imaging plate as a detector and Cu Kα radiation as an X-ray source (40 kV and 80 mA). The monofilament was arranged in the draw direction perpendicular to the X-ray beam, and the sample-to-detector distance was about 80 mm.

Indexing of the reflection spots and unit cell parameters were determined by a trial-and-error method. The unit cell parameters were refined by minimizing the sum of the square of the difference between the *d*-spacing (d_{obs}) calculated from the location of the diffraction spots and that (d_{cal}) calculated from the unit cell. The reliability parameter of indexing is expressed by the following equation:

$$R_{X-ray} = \left[\frac{\sum(d_{obs} - d_{cal})^2}{\sum d_{obs}}\right]^{1/2} \times 100\ (\%)$$

Two-dimensional intensity distribution data of X-ray fiber diagram were read out from the X-ray diffraction data on the image plate and then stored as pixel data (3000 × 3000 pixels, 100 μm a pixel) of Cartesian coordinates. The intensity of a diffraction spot is expressed as

$$I = ALp|F_{obs}|^2 \exp(-2B \sin^2\theta/\lambda^2)$$

where A, L, p, $|F_{obs}|$, and B are the X-ray absorption coefficient of the sample, the Lorentz factor, the polarization factor, the observed structure factor, and the isotropic temperature factor, respectively. The observed structure factors ($|F_{obs}|$) were calculated from the intensity measurements after removing the background intensity and correcting the Lorentz and polarization factors. The absorption effect was not taken into account in this study.

The X-ray diffraction patterns of melt-crystallized PCN films were obtained using a M18XHF diffractometer (MAC Science Co., Cu Kα radiation, 50 kV and 100 mA) at a scanning rate

Table 1. Characterization of PCN Samples

sample code	feed ratio of *trans*/*cis*-CHDM[a]	composition of *trans*/*cis*-CHDM in PCN[b]	T_m (°C)[c]	T_g (°C)[c]	intrinsic viscosity (dL/g)[d]
PCN-70	70.1/29.9	69.9/30.1	319.8	110.6	0.48
PCN-82	80.8/19.2	81.7/18.3	325.9	111.6	0.51
PCN-90	90.5/9.5	90.2/9.8	331.5	114.8	0.49
PCN-97	96.4/3.6	96.8/3.2	333.4	115.3	0.47

[a] Determined by gas chromatography. [b] Determined by ^{1}H NMR. [c] Determined by DSC for the melt-quenched amorphous samples. [d] Determined by Ubbelohde viscometer.

of 2°/min. The diffractometer was equipped with a $2\theta/\theta$ goniometer, a divergence slit (1.0°), a scattering slit (1.0°), and a receiving slit (0.30 mm). All X-ray measurements were performed at room temperature, and the sample-to-detector distance or *d*-spacing was calibrated using Si powder (2θ = 28.44°) as a standard.

Molecular Modeling. Conformational analysis and crystal structure modeling were carried out with the aid of molecular mechanics using a commercially available software Cerius[2] (version 4.0, Molecular Simulation Inc.) on a Silicon Graphics Indigo II workstation. The total potential energy of a molecular chain consists of contributions from intramolecular and intermolecular interactions. The intramolecular interactions consist of the bond stretching, valence angle bending, torsional, and inversion terms. The intermolecular interactions consist of van der Waals and Coulomb terms. The COMPASS force field[12] was used to calculate the potential energy of crystal structure, and the Ewald summation method was used in energy-minimizing calculations.[13−15] Standard bond lengths and angles for polyesters were adopted to build the repeating unit.

To obtain the useful conformational information such as local structure and chain flexibility of P*t*CN, conformational grid searches were performed by varying simultaneously the torsional angles of successive bonds and by plotting the total energy against each pair of rotational angles. In the grid scan method, the potential energy is calculated whenever a specific torsional angle is varied over a grid of an equally spaced value. When the rotations of two successive bonds are considered, the torsional angle of the first bond is fixed at a given value, and then the potential energies are calculated while the torsional angle of second bond is varied. For the conformational grid search, only one repeat unit of P*t*CN is considered, since we are only concerned with energies associated with torsional rotations of particular bonds.

In modeling of the crystal structure of P*t*CN, the length of repeating unit was adjusted to match it with the experimental *c*-axis. The chain was then translated and rotated within the unit cell in order to minimize the packing energy. During the energy minimization, the unit cell parameters were kept constant. The modeled structure factors ($|F_{mod}|$) were calculated using the atomic coordinates corresponding to the energy-minimized conformation of the chain in the unit cell. The scale factor and overall isotropic temperature factor were refined to minimize the difference between $|F_{mod}|$ and $|F_{obs}|$. The reasonability of the final crystal structure was evaluated by using the following reliability factor (*R*):

$$R = \frac{\sum ||F_{obs}| - |F_{mod}||}{\sum |F_{obs}|} \times 100\ (\%)$$

Results and Discussion

Effects of *Trans/Cis* Ratio of CHDM and Temperature on Crystal Structure of PtCN. Figure 3 shows X-ray fiber diagrams of PCNs prepared from CHDMs with different *trans*/*cis* isomer ratios. When the X-ray fiber diagrams are compared with each other, diffraction peak positions and intensities are very similar to one another. To investigate effects of the *trans*/*cis* ratio of the 1,4-cyclohexylenedimethyl group and crystallization temperature on the crystal structure

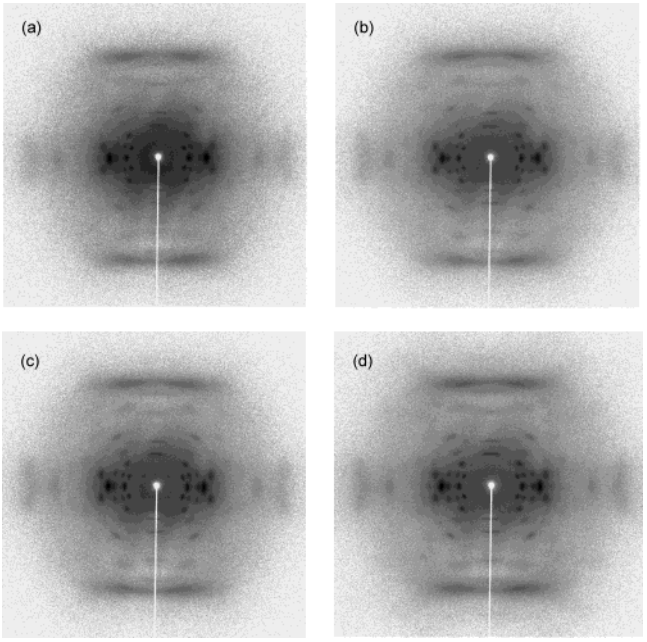

Figure 3. X-ray fiber diagrams of PCN monofilaments: (a) PCN-70; (b) PCN-82; (c) PCN-90; (d) PCN-97.

of P*t*CN, X-ray diffraction patterns for PCNs melt-crystallized at various crystallization temperatures are obtained. As can be seen in Figure 4, the diffraction pattern of PCN-97 is nearly the same as that of PCN-70, indicating that incorporation of a small amount of *cis*-CHDM does not significantly change the crystal structure of P*t*CN. When the *d*-spacings of PCN-97 and their variation by change of the crystallization temperature are compared with those of PCN-70 and PCN-81, it also reveals that the *d*-spacings of each reflection and their variations with the crystallization temperature remain nearly unchanged, as shown in Figure 5. Therefore, we identify the crystal structure of PCN-97 with that of P*t*CN in this study. It is noted that Boye[16] have reported that PCT with a 68% *trans* isomer also crystallizes with a unit cell much the same as that of poly(1,4-*trans*-cylcohexylenedimethylene terephthalate) (P*t*CT).

Crystal Structure Determination by X-ray Fiber Diffraction. The distance between diffraction layers including the equatorial line, determined from the X-ray fiber diagram (Figure 3d), was 1.66 nm, which corresponds to the crystallographic repeat length of the unit cell. Since the fiber repeat length of 1.66 nm is nearly identical with the chemical repeat length (1.68 nm) of the fully extended conformation of P*t*CN backbone with the chair form of cyclohexane unit, it seems reasonable to assume that the cycloaliphatic groups are in fully extended conformation and that cyclohexane rings are in the chair form. All the diffraction spots observed in the X-ray fiber diagram are identified, as listed in Table 2, and compared with a triclinic unit cell with dimen-

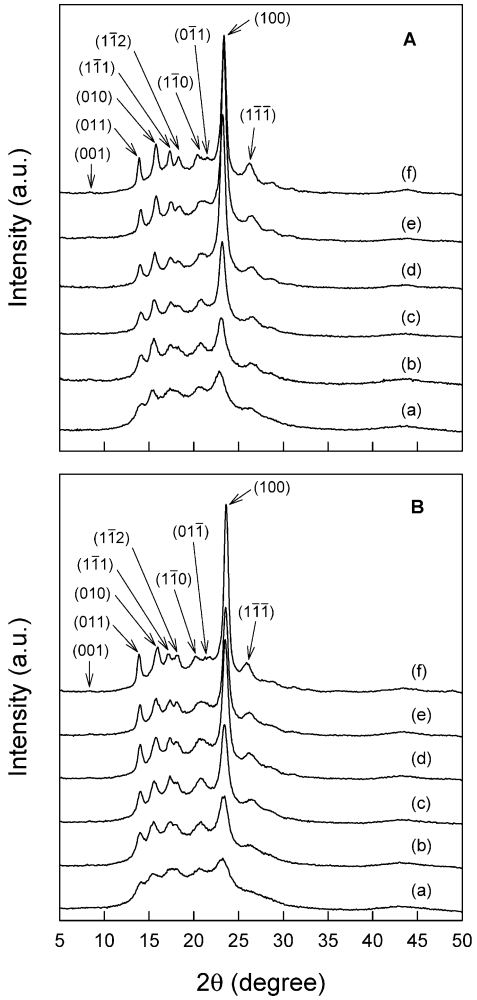

Figure 4. X-ray diffraction patterns of (A) PCN-70 and (B) PCN-97 samples melt-crystallized at various crystallization temperatures: (a) 150, (b) 180, (c) 210, (d) 240, (e) 270, and (f) 300 °C.

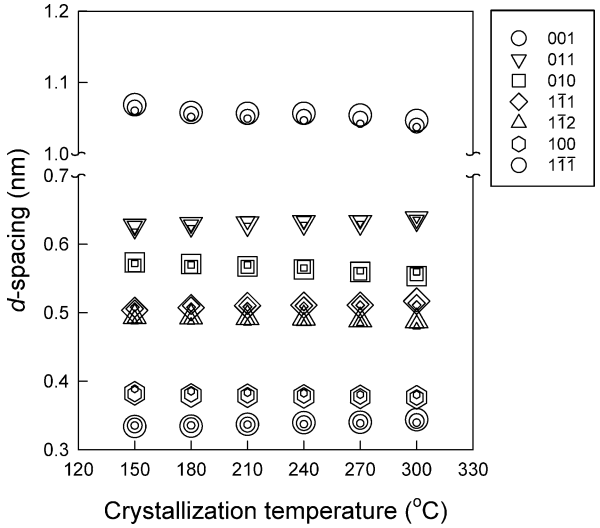

Figure 5. Change of *d*-spacings with the crystallization temperature for PCN-70, PCN-80, and PCN-97. The small, medium, and large symbols denote PCN-70, PCN-80, and PCN-97, respectively.

sions of $a = 0.638$ nm, $b = 0.657$ nm, $c = 1.661$ nm, $\alpha = 83.41°$, $\beta = 43.92°$, and $\gamma = 106.02°$. The reliability parameter of indexation (R_{X-ray}) was 1.47% after refinement of the unit cell dimension, indicating that the

Table 2. Comparison of Calculated *d*-Spacings and Structure Factors of P*t*CN with Observed Ones

hkl	d_c/Å	d_o/Å	$\lvert F_{mod.ref}\rvert$	$\lvert F_{mod}\rvert^a$	$\lvert F_{obs}\rvert$
010	5.587	5.597	39.28		36.18
1$\bar{1}$0	4.351	4.341	26.20		36.27
100	3.776	3.754	102.26		103.57
1$\bar{2}$0	3.168	3.175	23.73		28.94
020	2.793	2.807	14.75		15.37
110	2.569	2.541	17.78		16.63
1$\bar{3}$0	2.180	2.179	27.83	36.04	39.65
2$\bar{2}$0	2.175		22.90		
2$\bar{3}$0	1.914	1.882	26.35	49.12	53.92
200	1.888		32.56		
030	1.862		25.66		
001	10.169	10.285	4.93		6.51
011	6.305	6.295	35.93		41.24
1$\bar{1}$1	5.127	5.094	25.74	27.25	34.61
101	5.078		8.96		
01$\bar{1}$	4.143	4.178	43.60		35.78
1$\bar{1}$$\bar{1}$	3.391	3.347	72.32		53.12
10$\bar{1}$	2.877	2.860	22.29		26.66
02$\bar{1}$	2.419	2.401	18.37	32.71	36.73
2$\bar{2}$1	2.411		27.06		
11$\bar{1}$	2.138	2.129	33.47		28.29
2$\bar{2}$$\bar{1}$	1.925		17.89		
2$\bar{1}$$\bar{1}$	1.860	1.850	57.76		53.28
012	5.156	5.153	23.58		18.47
002	5.084		8.88		
1$\bar{1}$2	4.846	4.885	32.59		26.81
022	3.153	3.127	12.85	28.37	31.57
01$\bar{2}$	3.103		25.29		
2$\bar{1}$2	2.868		12.06		
1$\bar{1}$2	2.668	2.654	34.28		31.42
202	2.539		16.90		
122	2.310		15.17		
103	5.415	5.439	12.70		15.43
113	3.898	3.895	12.17	20.30	16.12
1$\bar{1}$3	3.879		7.81		
013	3.796		14.25		
2$\bar{1}$3	3.094	3.075	12.74		14.47
104	4.056	4.022	7.67		9.05
114	3.629	3.616	11.51		9.83
2$\bar{1}$4	3.062	3.034	21.02	25.95	21.59
1$\bar{1}$4	3.019		15.21		
014	2.880		12.57		
004	2.542	2.544	16.85		19.43
3$\bar{1}$4	2.025		15.93		
034	2.023		15.57		
224	1.825		16.65		
205	2.987		7.85		
125	2.439	2.413	23.26		19.18
2$\bar{2}$5	2.190	2.195	18.15		17.41
3$\bar{2}$5	1.979		22.10		
035	1.884		20.82		
135	1.842		28.28		
206	2.707	2.692	19.52		15.25
116	2.547	2.520	11.54		8.75
216	2.441	2.428	24.42	30.55	27.58
106	2.410		18.35		
126	2.234	2.217	24.11		20.03
226	1.949		18.69		
3$\bar{2}$6	1.918		25.03		
316	1.763		27.08		
217	2.265	2.238	24.41		18.54
11$\bar{7}$	2.121		10.72		
2$\bar{1}$7	2.088	2.080	51.00		40.93
3$\bar{1}$7	2.026	1.990	31.97	56.41	49.14
127	1.992		32.46		
227	1.911		33.26		
317	1.802		20.34		
2$\bar{2}$7	1.708		16.92		
1$\bar{1}$7	1.677		35.38		
208	2.028	2.019	10.15		14.81
3$\bar{1}$8	1.883	1.880	19.89		15.29
228	1.814	1.802	15.79	20.43	24.90
2$\bar{1}$8	1.799		12.15		
118	1.797		4.54		
128	1.760	1.759	21.26		15.82

[a] $\lvert F_{mod}\rvert = (\Sigma\lvert F_{mod.ref}\rvert^2)^{1/2}$ for overlapping reflections.

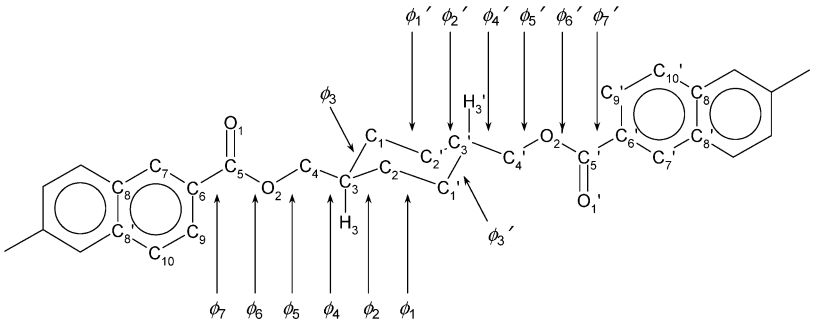

Figure 6. Numbering of atoms and torsion angles in P*t*CN.

identification of the unit cell is quite satisfactory. The crystal density calculated from the unit cell parameters is 1.313 g/cm^3, which is very close to the experimental value (1.315 ± 0.003 g/cm^3) as estimated using the following equations:

$$\frac{1}{\rho} = \frac{x_c}{\rho_{cr}} + \frac{1 - x_c}{\rho_{am}}$$

where x_c, ρ, ρ_{cr}, and ρ_{am} are the degree of crystallinity determined by X-ray measurement, the density of sample, the density of crystalline phase, and the density of amorphous phase, respectively. The density (ρ_{am}) of amorphous PCN-97 sample was 1.284 ± 0.002 g/cm^{-3}.

From comparison of the measured crystal density with the calculated one and of the crystallographic length of *c*-axis with the chemical repeat length, it is realized that single polymer chain passes through an *a*−*b* plane of the unit cell. Since both the center of the cyclohexyl group and the midpoint of naphthaloyl group of P*t*CN backbone in the triclinic unit cell are crystallographic centers of symmetry, the space group is identified as $P\bar{1}$. Therefore, all of the bond lengths, bond angles, and torsion angles in polymer backbone are symmetric on the basis of these centers of symmetry.

Molecular Modeling of Crystal Structure. The chemical repeat unit of P*t*CN is illustrated in Figure 6, where the numbering of the atoms and torsion angles are designated. The contour maps of conformational energy with respect to the torsional angles of successive bonds (ϕ_4 vs ϕ_5 and ϕ_5 vs ϕ_6) are shown in Figure 7, from which it is realized that torsional angles of ϕ_4, ϕ_5, and ϕ_6 are around 180°; i.e., all the bonds take the *trans* conformation. On the basis of the fact that 1,4-*trans*-cyclohexylenedimethyl group and the naphthaloyl group lie on crystallographic centers of symmetry, the initial molecular model of P*t*CN satisfying the constraint such as the length of crystallographic *c*-axis was generated and inserted in the unit cell. Subsequently, a molecular mechanics calculation was performed by minimizing the total energy of the unit cell with respect to intramolecular and intermolecular energy. As a result, the most energy-minimized crystal structure was obtained, and then the structure factors calculated from the modeled crystal structure are compared with the experimentally observed structure factors. The observed and modeled structure factors of all the diffraction spots examined are listed in Table 2. The *R* factor obtained by comparing the observed structure factors ($|F_{obs}|$) with modeled ones ($|F_{mod}|$) is 16.2%. In this refinement, the overall isotropic temperature factor was 5.7 Å^2. When the simulated X-ray fiber diagram is compared with the experimentally obtained X-ray fiber diagram, the two diagrams are found nearly identical, as shown in Figure 8. The bond lengths and bond angles of the final structural model are listed in Table 3, and the torsion angles are determined to be ϕ_1 = C3′−C1′−C2−C3 = $-\phi_1'$ = −54.7°, ϕ_2 = C1′−C2−C3−C4 = $-\phi_2'$ = 178.7°, ϕ_3 = C2′−C1−C3−C4 = $-\phi_3'$ = −178.7°, ϕ_4 = C1−C3−C4−O2 = $-\phi_4'$ = 179.3°, ϕ_5 = C3−C4−O2−C5 = $-\phi_5'$ = 177.0°, ϕ_6 = C4−O2−C5−C6 = $-\phi_6'$ = 174.0°, and ϕ_7 = O2−C5−C6−C7 = $-\phi_7'$ = −173.5°. The carboxylic groups in the P*t*CN backbone are nearly coplanar to the naphthalene ring plane, and the cyclohexane unit is in the chair conformation. The energy-minimized molecular packing in the unit cell is shown in Figure 9, from which it is clear that the naphthalene groups are in a face-to-face arrangement. Fractional coordinates of each atom in the unit cell are listed in Table 4.

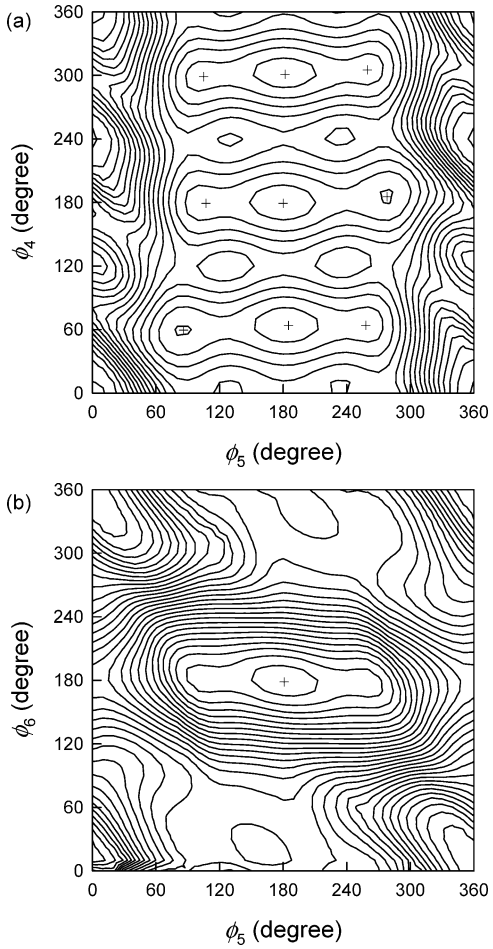

Figure 7. Contour maps of conformational energy calculated for each pair of dihedral angles of P*t*CN backbone shown in Figure 6. Energy contour lines are drawn every 1 kcal/mol, and local minima of energy are marked by the (+) sign.

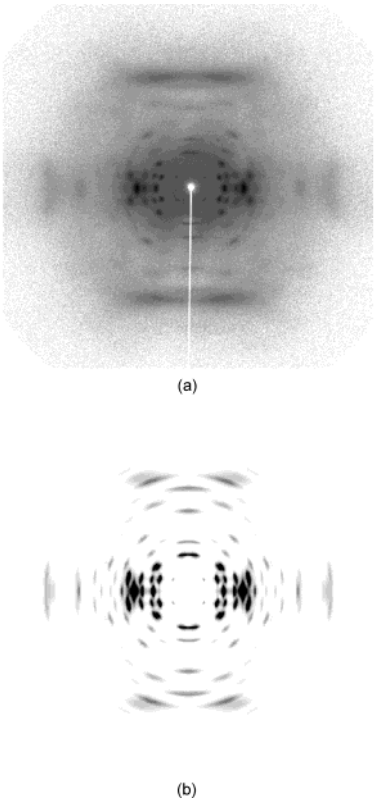

Figure 8. Comparison of (a) experimental X-ray fiber diagram of PCN-97 with (b) simulated X-ray fiber diagram, where the angular deviation from perfect orientation is 4°.

Table 3. Bond Lengths and Bond Angles in P*t*CN

bond length (Å)		bond angle (deg)	
bond	length	bonds	angle
C1−C2′	1.535	C1′−C2−C3	112.2
C1−C3	1.387	C2′−C1−C3	111.1
C2−C3	1.540	C1−C3−C4	110.5
C3−C4	1.533	C2−C3−C4	111.5
C4−O2	1.499	C3−C4−O2	110.6
O2−C5	1.366	C4−O2−C5	119.6
C5−O1	1.214	O2−C5−C6	110.0
C5−C6	1.428	C5−C6−C9	122.6
C6−C7	1.387	C7−C6−C9	119.4
C6−C9	1.404	C6−C7−C8	121.3
C7−C8	1.410	C6−C9−C10	121.3
C8−C8′	1.436	C7−C8−C8′	121.6
C9−C10	1.377	C8−C8′−C10	114.8
C10−C8′	1.482	C8′−C10−C9	121.6

It is worthy to note that the crystal structure of P*t*CN is similar to that of P*t*CT.[16,17] Therefore, it is likely expected that the crystal structure of P*t*CN is not significantly changed when the naphthalene ring in P*t*CN is replaced by a benzene ring. This leads us to expect that the random copolyesters composed of 1,4-cyclohexylenedimethylene terephthalate and 1,4-cyclohexylenedimethylene 2,6-naphthalate units show cocrystallization behavior. This cocrystallization behavior will be reported in the near future.

Conclusions

As a primary study of PCN, the crystal structure of P*t*CN was identified by using X-ray fiber diffraction and molecular modeling. The unit cell of P*t*CN was found to be a triclinic with dimensions of $a = 0.638$ nm, $b = 0.657$ nm, $c = 1.661$ nm, $\alpha = 83.41°$, $\beta = 43.92°$, and $\gamma = 106.02°$. The calculated crystal density of 1.313 g/cm^3 indicates that there is one repeating unit in a unit cell. The repeat unit of P*t*CN in a triclinic unit cell possess two crystallographic centers of symmetry (space group $P\bar{1}$). It is also identified that cycloaliphatic unit is in the *all-trans* conformation and that the *trans*-1,4-cyclohexylenedimethyl group, $-O-CH_2-(C_6H_{10})-CH_2-O-$, is in the conformation of t^t_{+g} $(t \pm gt)^{-g}_t t$ (*g*, *gauche*; *t*, *trans*) in the P*t*CN unit cell. The energy-minimized molecular packing in the unit cell shows that neighbor-

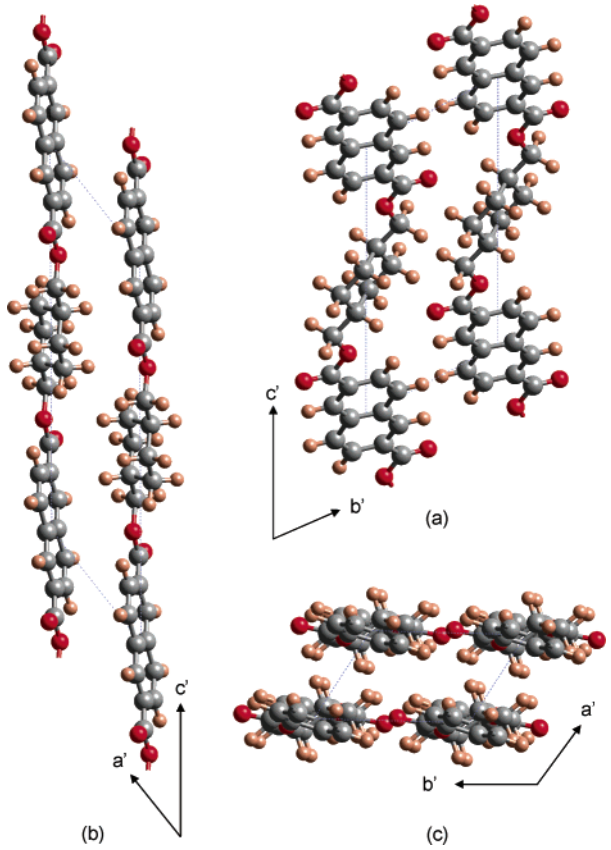

Figure 9. Molecular packing of P*t*CN backbone in triclinic unit cell: (a) projection along *a*-axis; (b) projection along *b*-axis; (c) projection along *c*-axis.

Table 4. Fractional Atomic Coordinates of P*t*CN

atom	*x*/*a*	*y*/*b*	*z*/*c*
C1	0.0832	−0.1901	0.4938
C2	−0.1353	0.0190	0.4593
C3	0.1168	−0.0768	0.4005
C4	0.0556	−0.2516	0.3570
C5	0.0228	−0.2690	0.2180
C6	0.0297	−0.1339	0.1417
C7	−0.0646	−0.2477	0.0988
C8	−0.0561	−0.1246	0.0204
C9	0.1327	0.1083	0.1074
C10	0.1467	0.2358	0.0305
O1	−0.0344	−0.4714	0.2464
O2	0.0850	−0.1378	0.2635
H1[a]	−0.1841	−0.3518	0.5801
H1′[a]	0.2738	−0.2500	0.4498
H2	−0.4113	−0.1332	0.5432
H2′	−0.0980	0.1106	0.3866
H3′	0.3906	0.0778	0.3117
H4	0.2500	−0.3084	0.3087
H4′	−0.2087	−0.4143	0.4435
H7	−0.1520	−0.4382	0.1261
H9	0.2047	0.2029	0.1413
H10	0.2325	0.4259	0.0039

[a] H1 and H1′ mean hydrogens that are covalent-bonded to C1.

ing naphthalene rings are in the face-to-face arrangement.

Acknowledgment. The authors thank the Korea Science and Engineering Foundation (KOSEF) for financial support through the Hyperstructured Organic Materials Research Center (HOMRC).

References and Notes

(1) Duling, I. N.; Chester, W. U.S. Patent 3,436,376, Apr 1, 1969.
(2) Mencik, Z. *Chem. Prum.* **1967**, *17*, 78.
(3) Liu, J.; Myers, J.; Geil, P. H.; Kim, J. C.; Cakmak, M. *SPE Antec. Technol.* **1997**, 43.
(4) Buchner, S.; Wiswe, D.; Zachmann, H. G. *Polymer* **1989**, *30*, 480.
(5) Watanabe, H. *Kobunshi Ronbunshu* **1976**, *33*, 299.
(6) Koyano, H.; Yamamoto, Y.; Saito, Y.; Yamanobe, T.; Komoto, T. *Polymer* **1998**, *39*, 4385.
(7) Jeong, Y. G.; Jo, W. H.; Lee, S. C. *Proc. Korean Textile Conf.* **1999**, *32* (2), 307.
(8) Jeong, Y. G.; Jo, W. H.; Lee, S. C. *Polymer* **2002**, *43*, 7315.
(9) Jeong, Y. G.; Jo, W. H.; Lee, S. C. *Polym. J.* **2001**, *12*, 913.
(10) Jeong, Y. G.; Jo, W. H.; Lee, S. C. Unpublished data.
(11) Yohiaki, T.; Susumi, Y.; Naoki, O.; Yoshibumi, I.; Kazuaki, K. U.S. Patent 4,999,090, Mar 1, 1991.
(12) Sun, H. *J. Phys. Chem. B* **1998**, *102*, 7338.
(13) Ewald, P. P. *Ann. Phys.* **1921**, *64*, 253.
(14) Karasawa, N.; Goddard, W. A., III. *J. Phys. Chem.* **1989**, *93*, 7320.
(15) Jang, S. S.; Jo, W. H. *Fibers Polym.* **2000**, *1*, 18.
(16) Boye, C. A. *J. Polym. Sci.* **1961**, *55*, 275.
(17) Remillard, B.; Brisse, F. *Polymer* **1982**, *23*, 1960.

MA0215666